

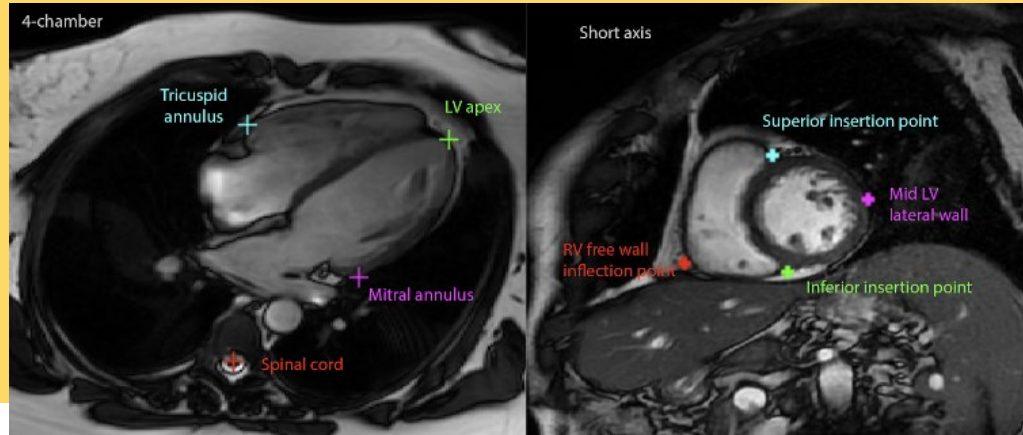
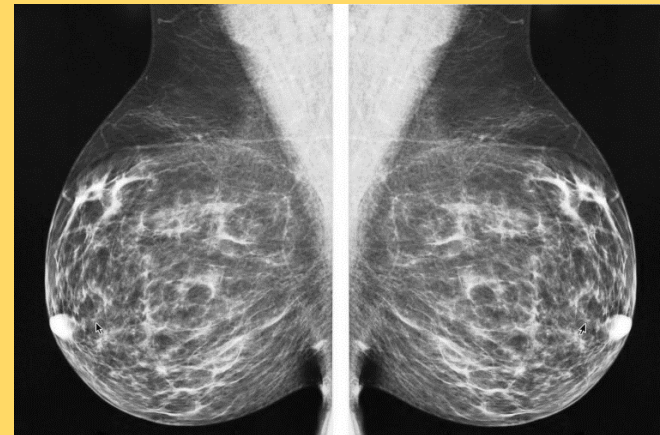
Machine Learning and Medical Imaging

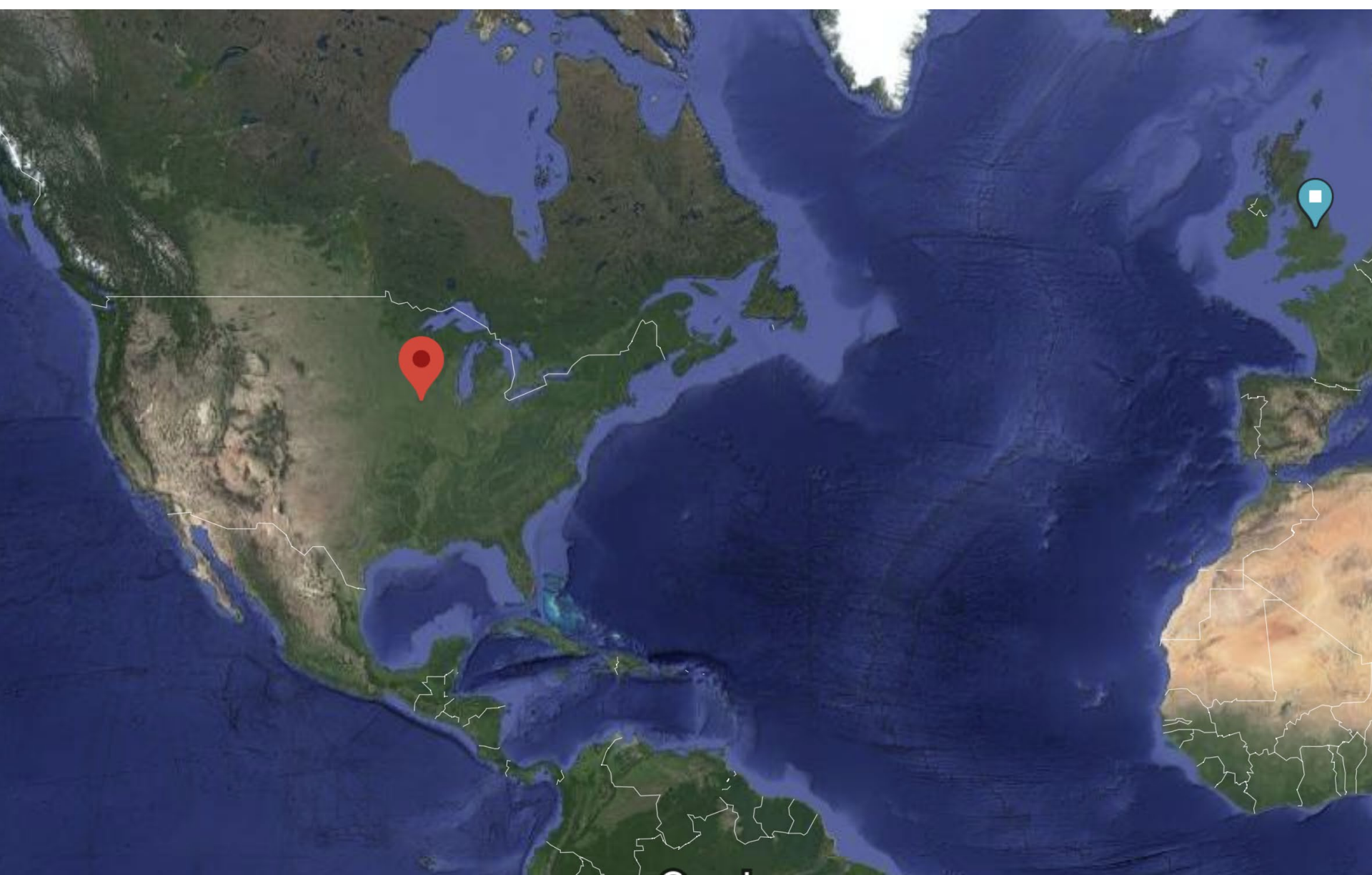
Johanna Uthoff, PhD



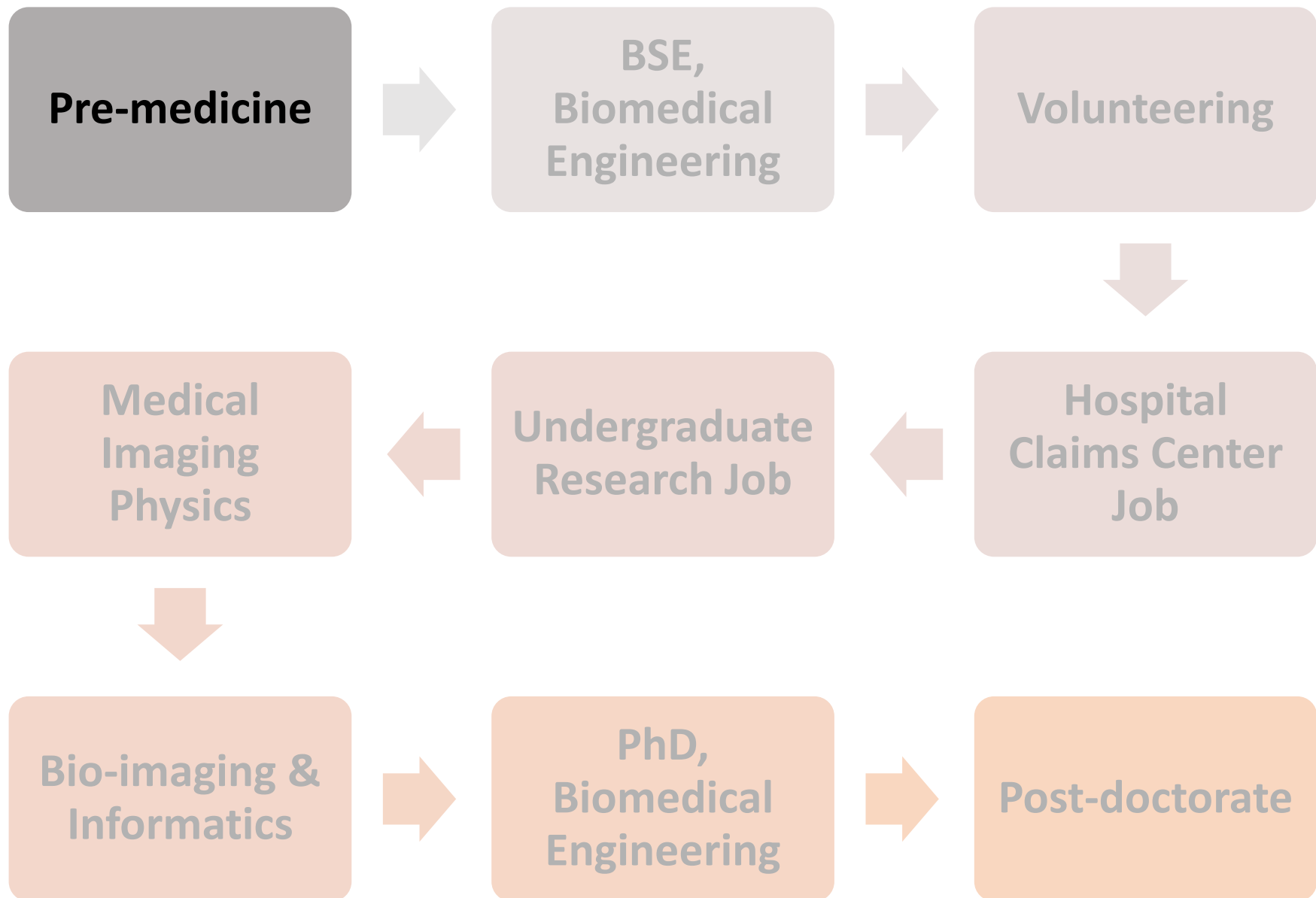
Lecture Overview

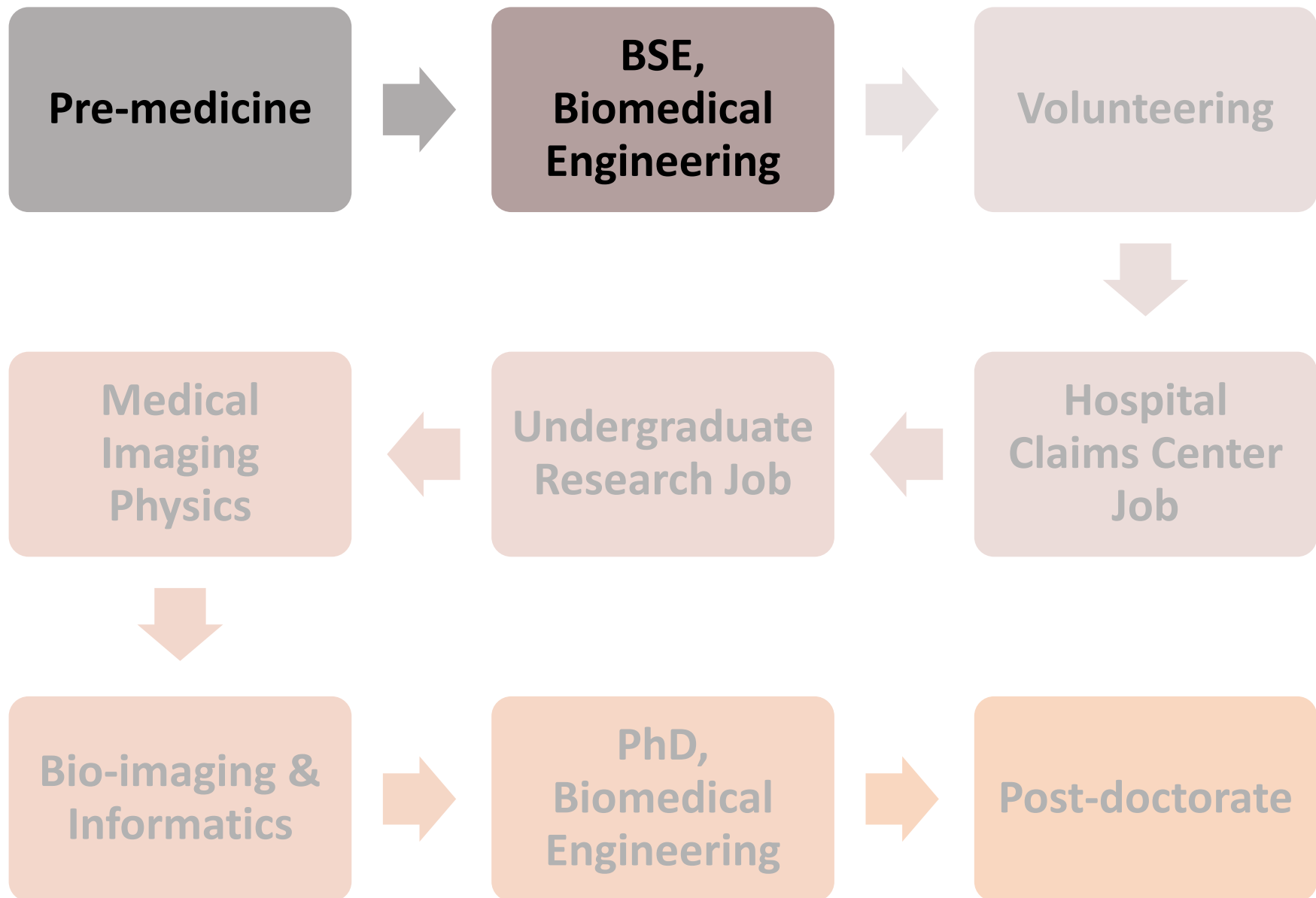
1. My Journey
2. Medical Imaging
3. Applications
 1. Lung Cancer (CT)
 2. Breast Cancer (MG)
 3. Pulmonary Hypertension (MRI)
4. Considerations

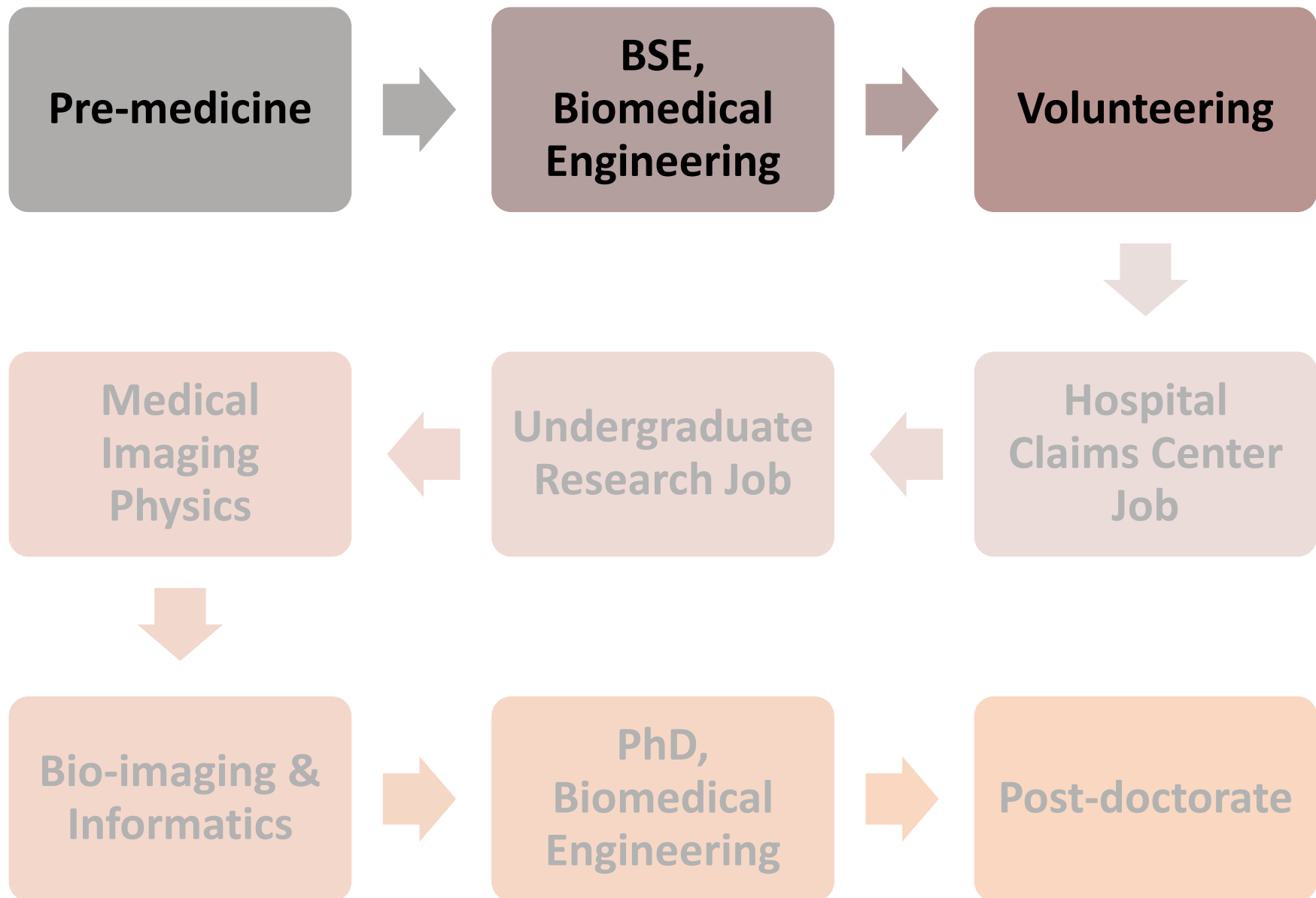


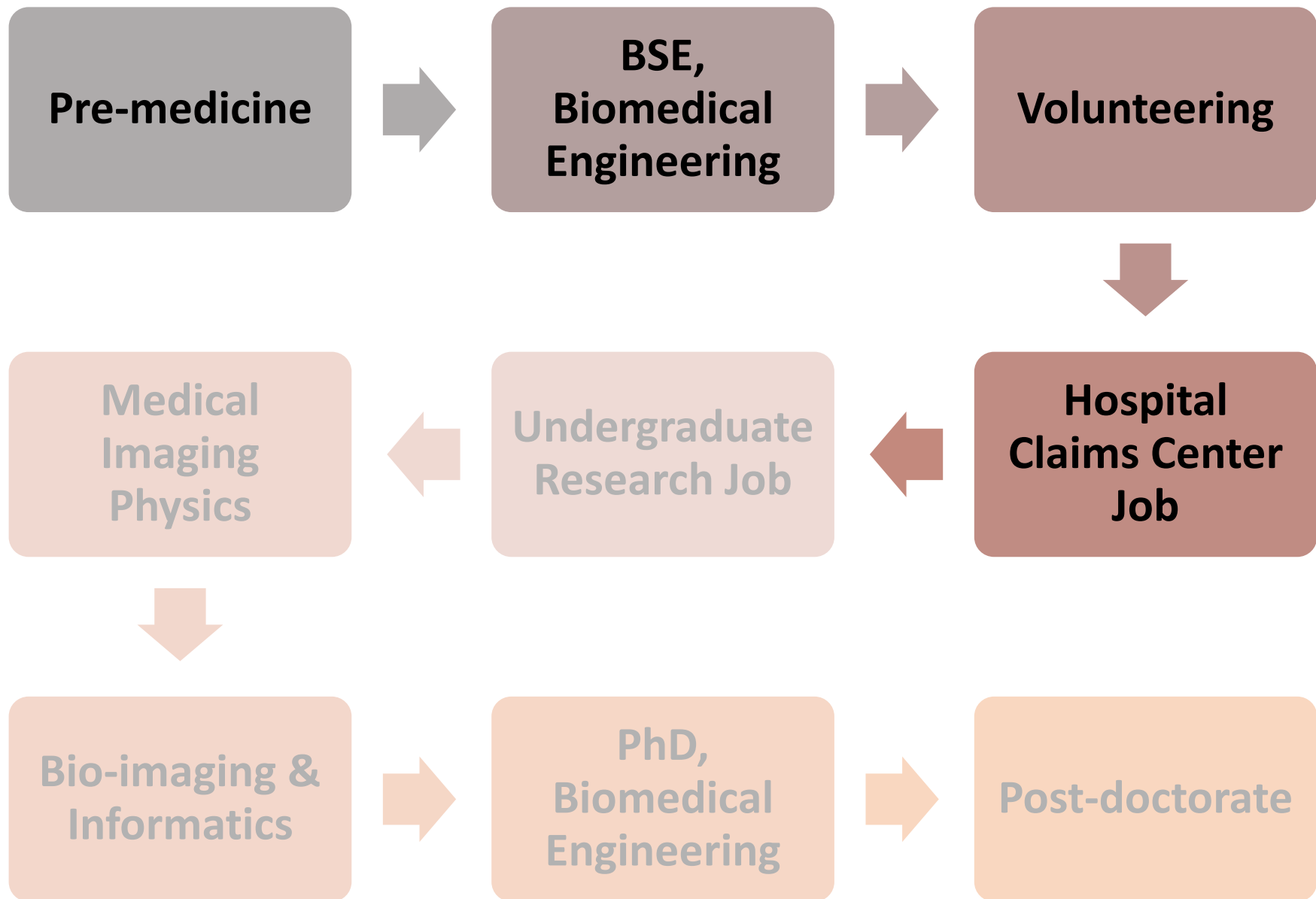


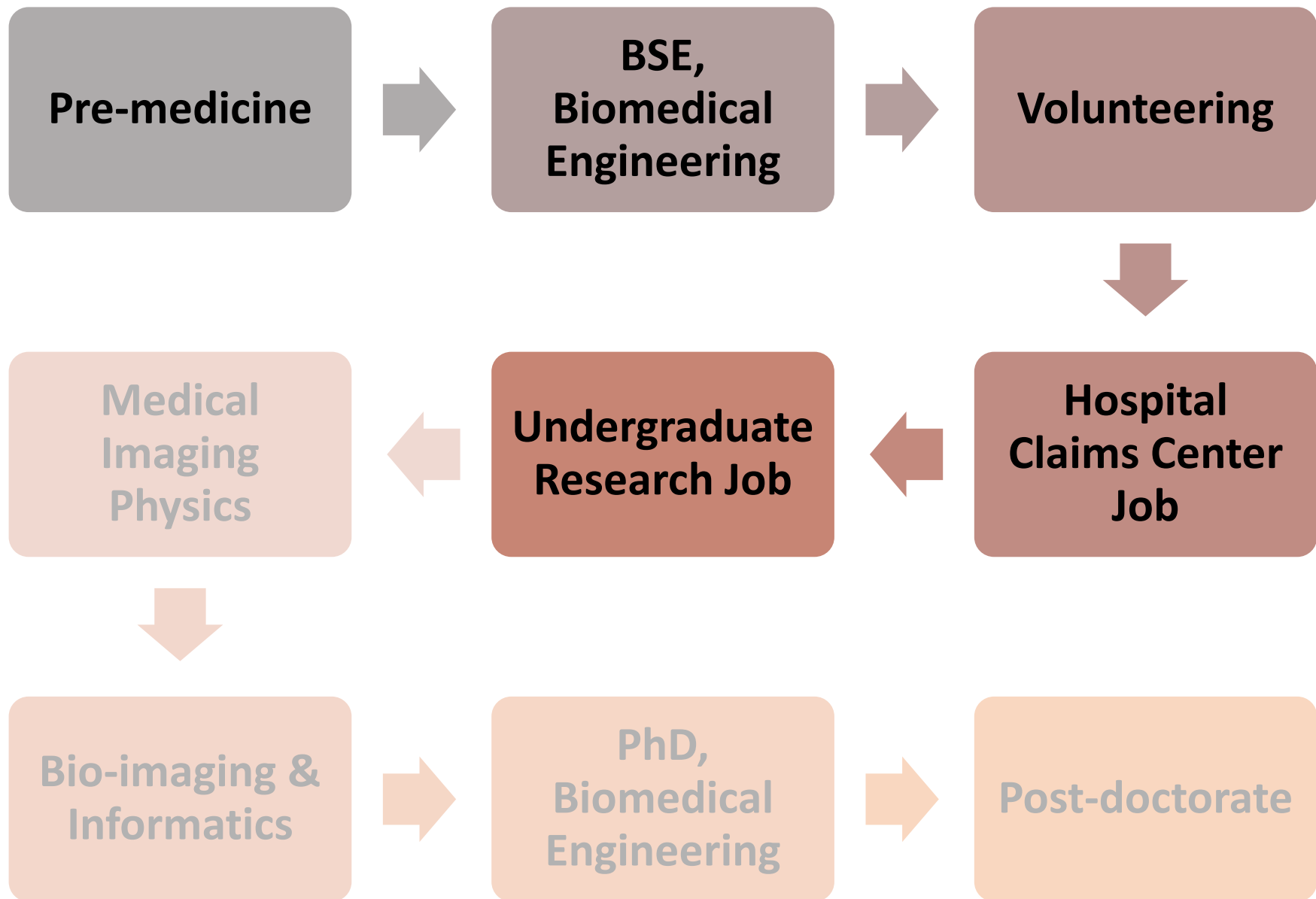


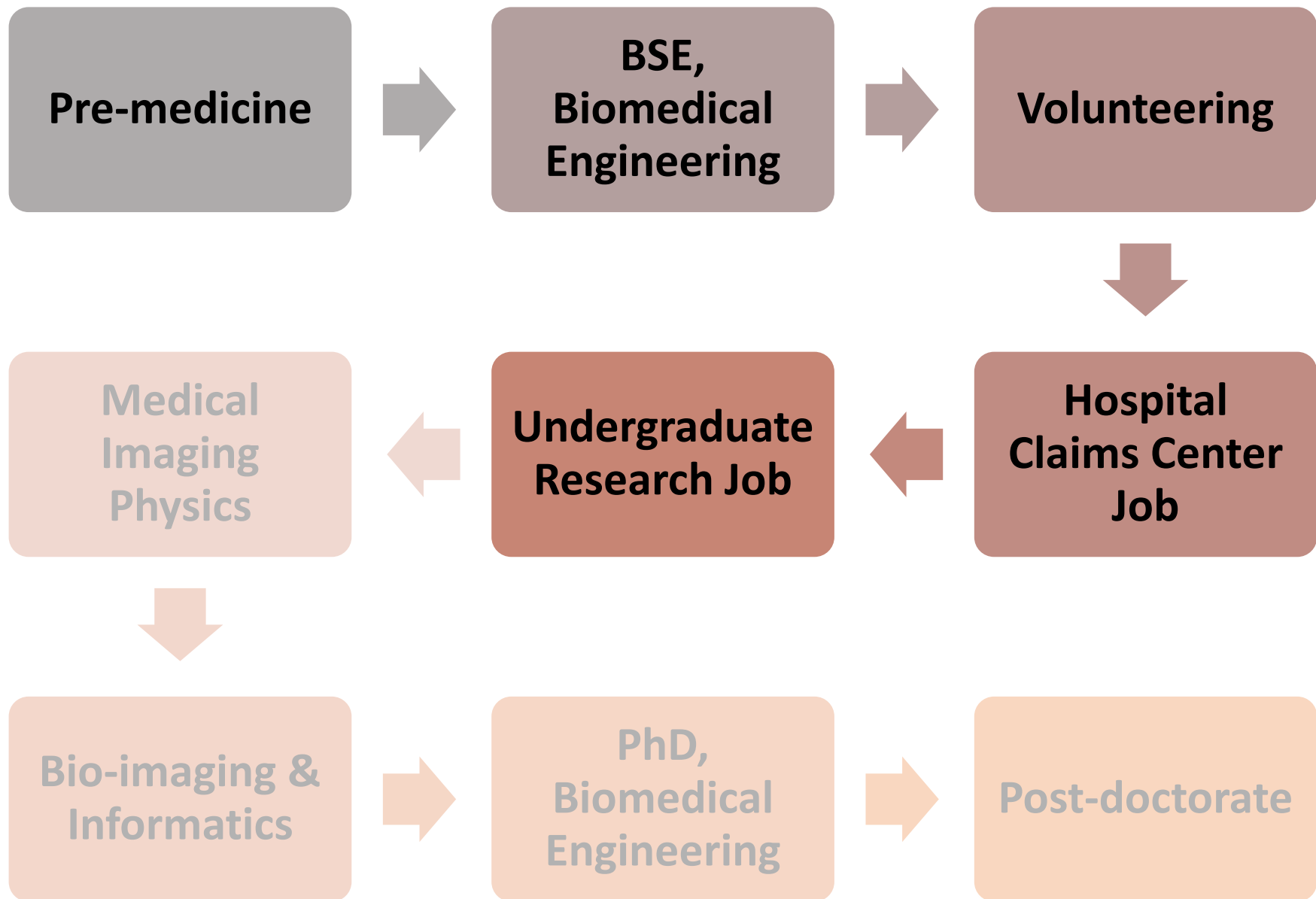


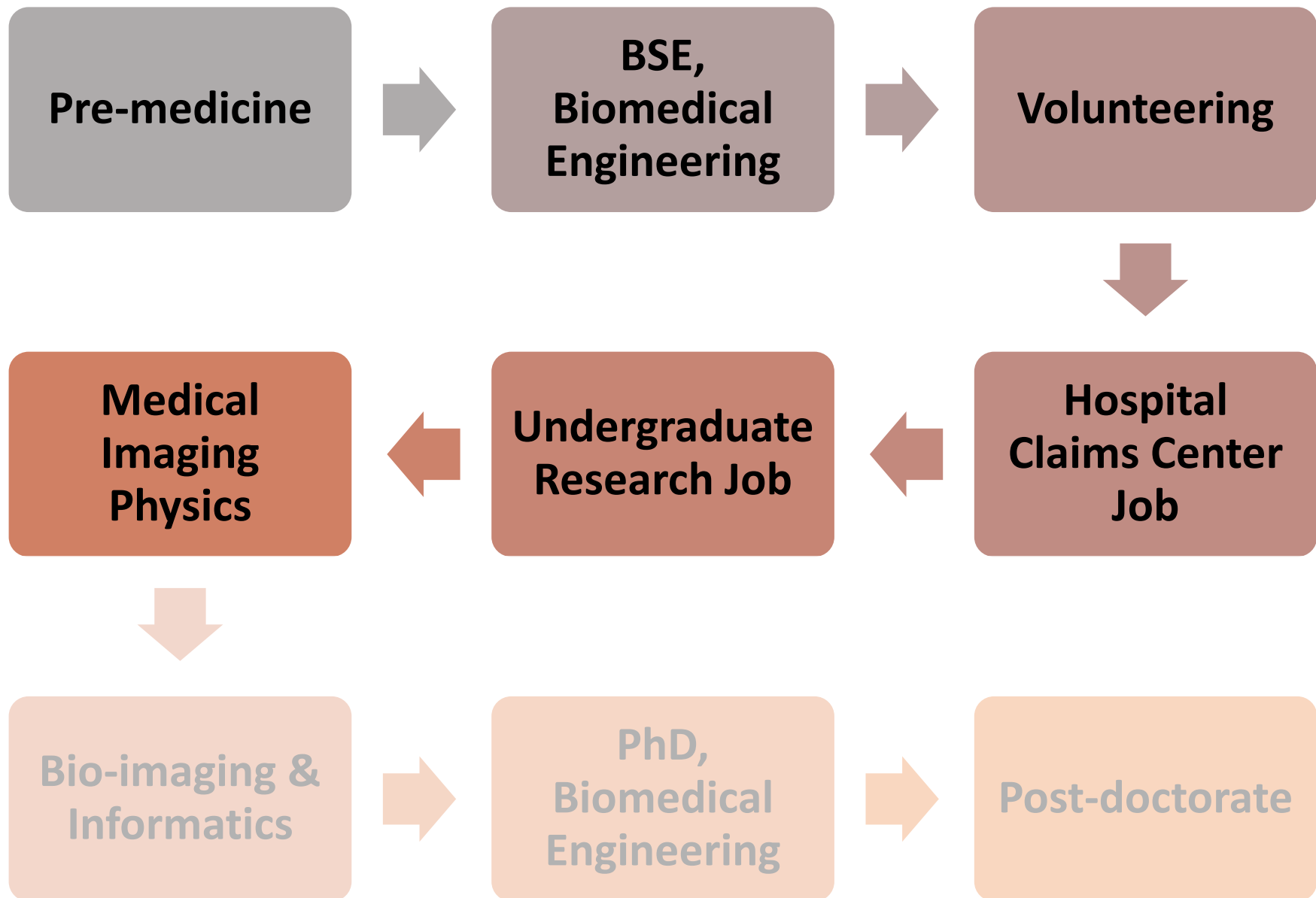


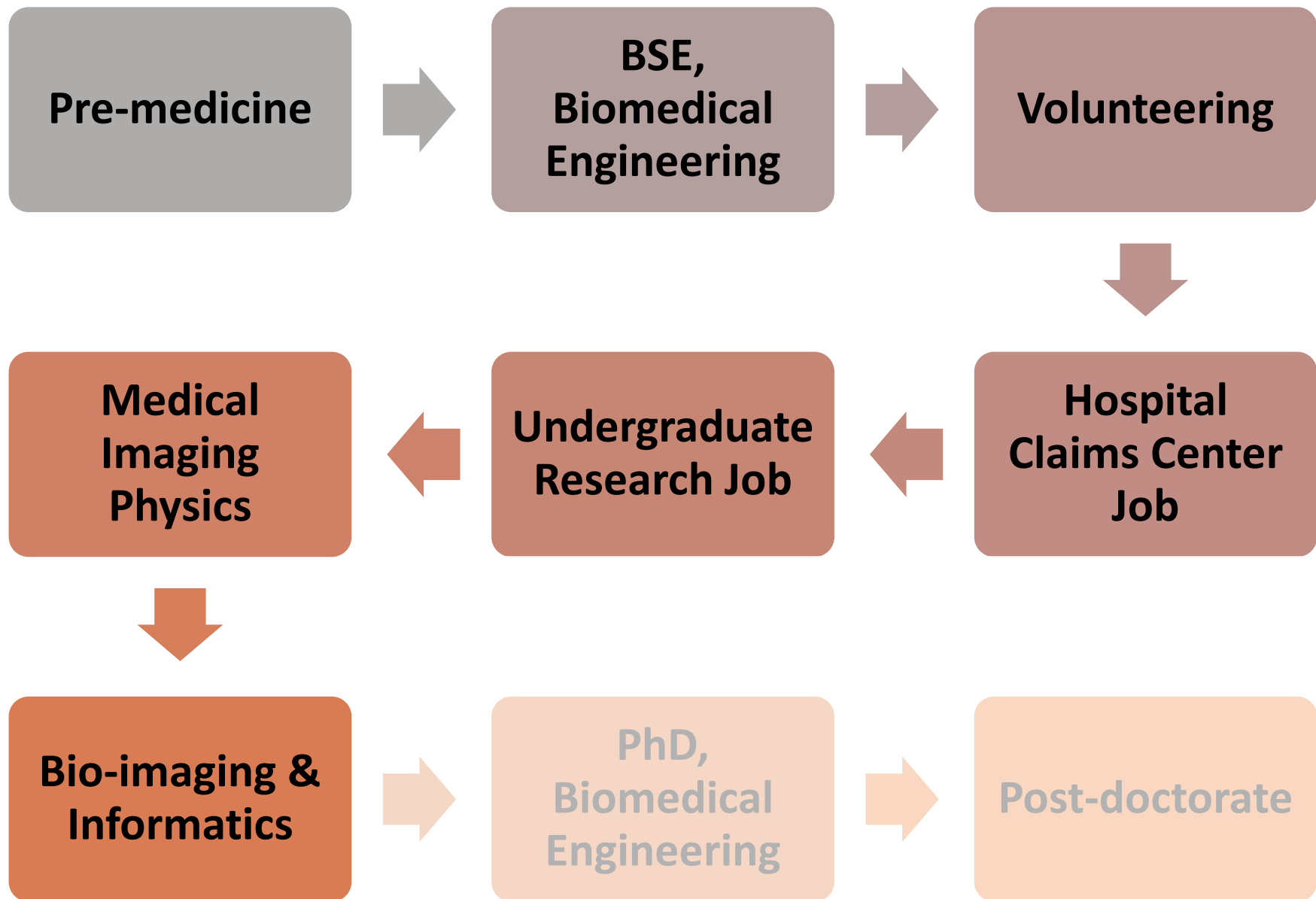


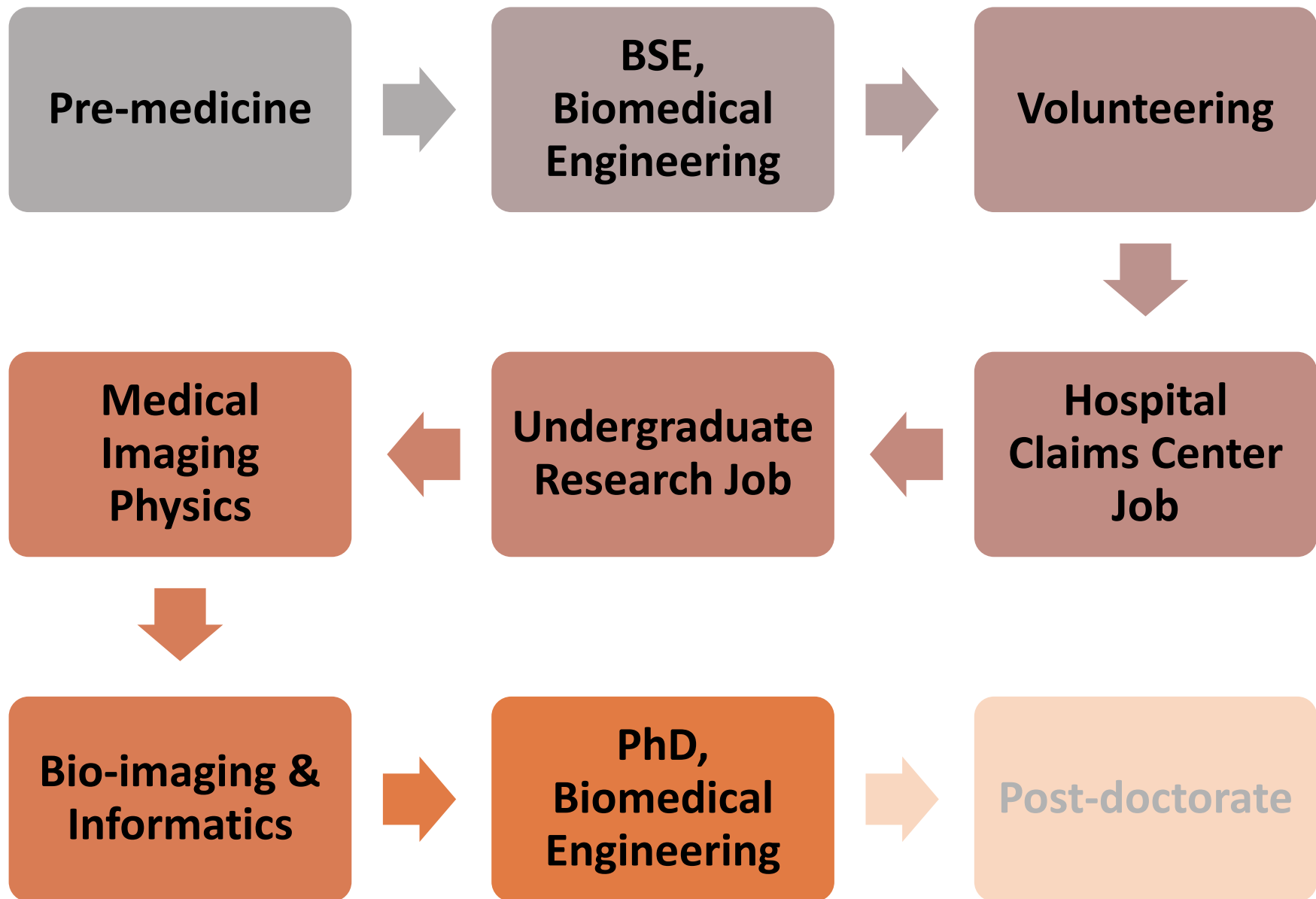


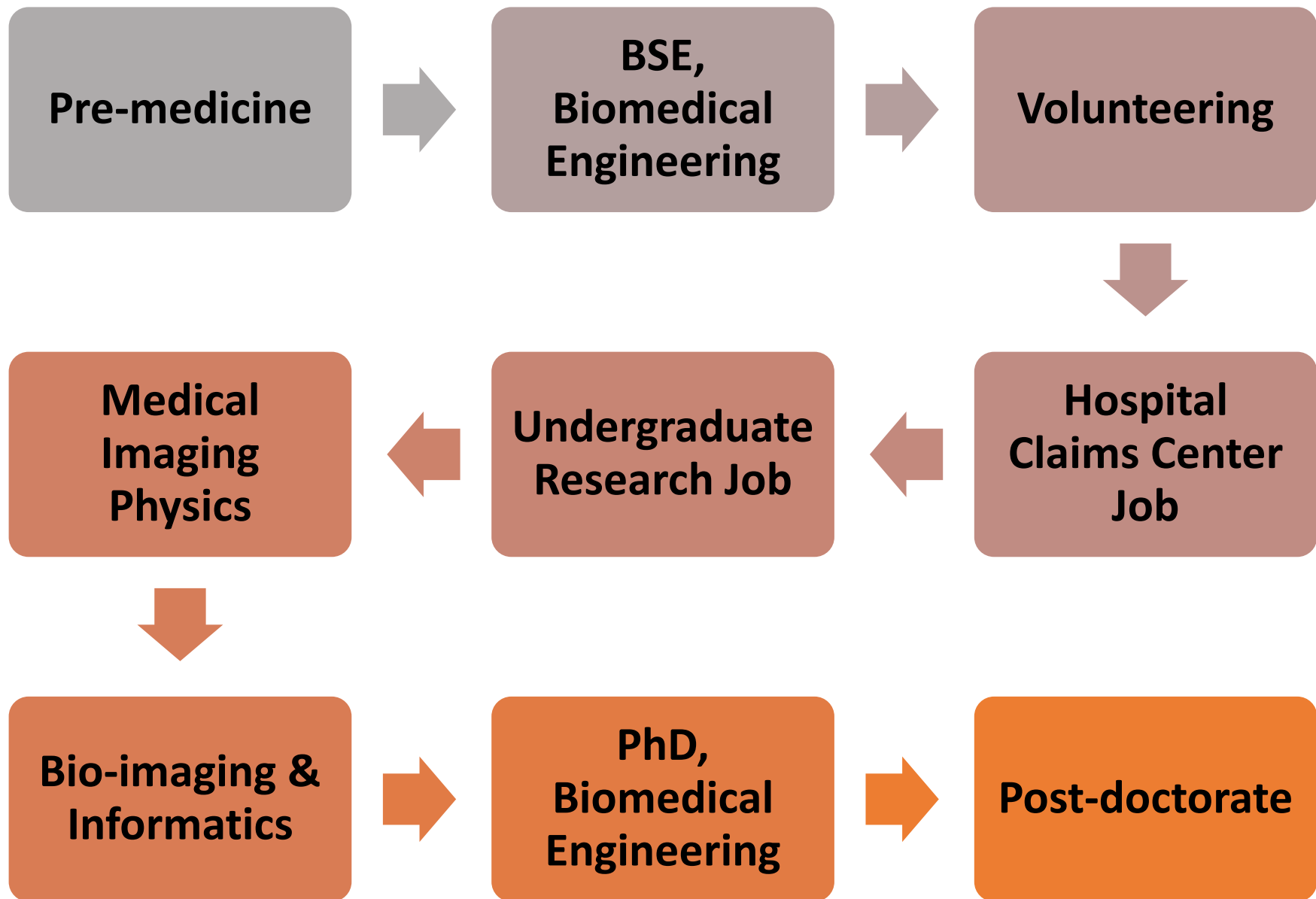


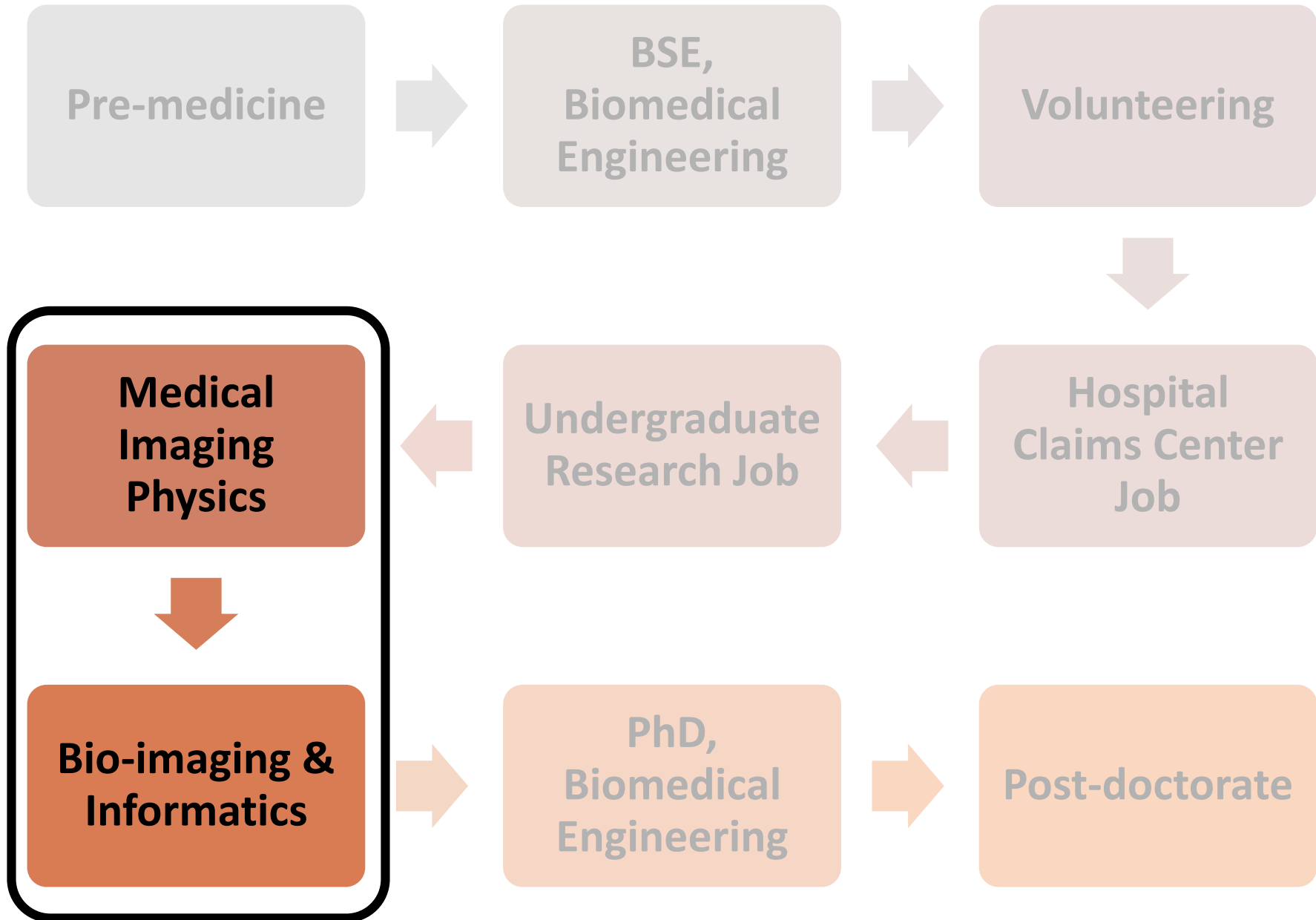




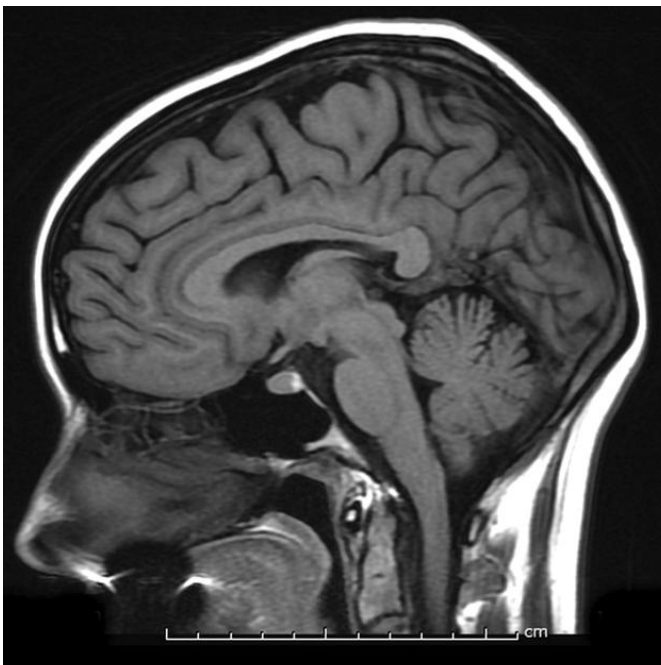
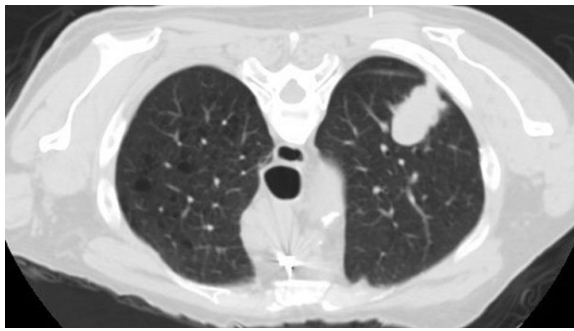
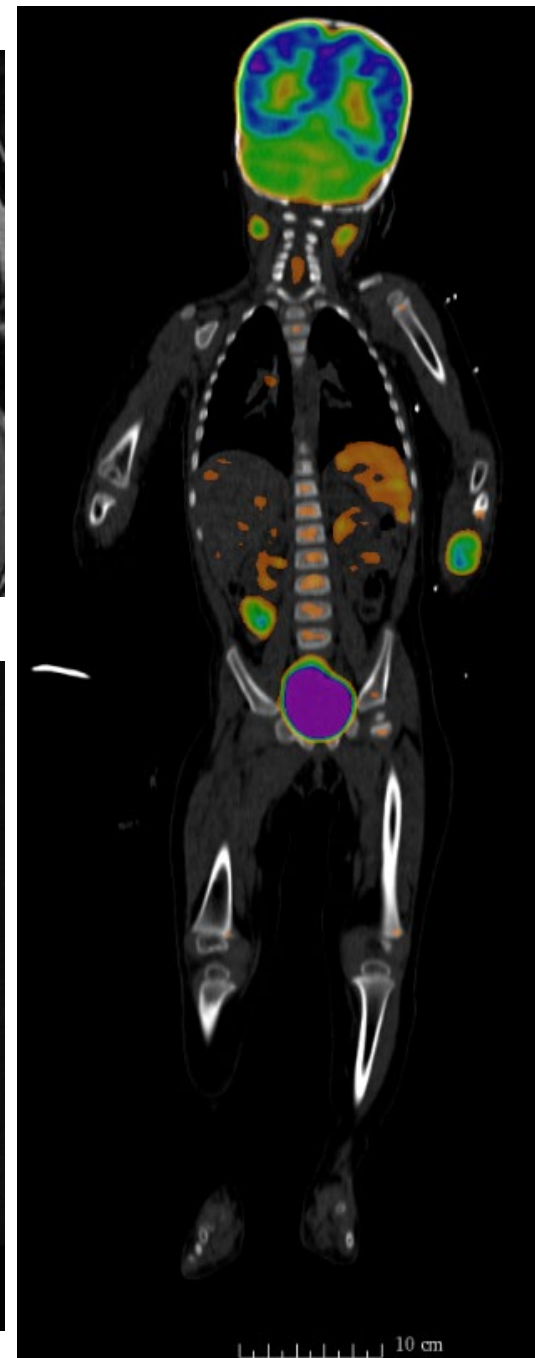
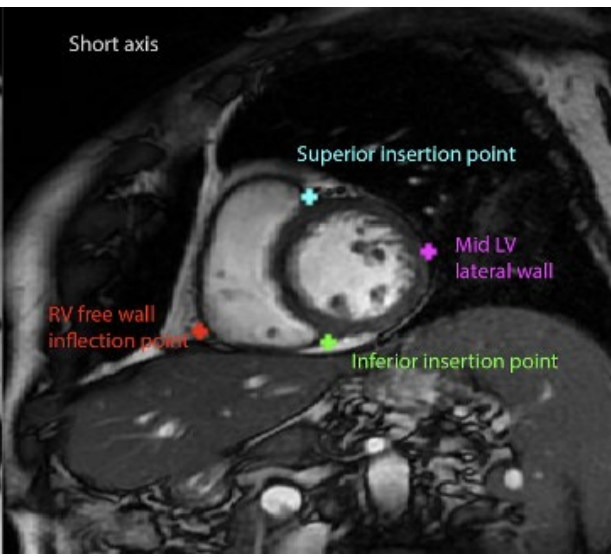
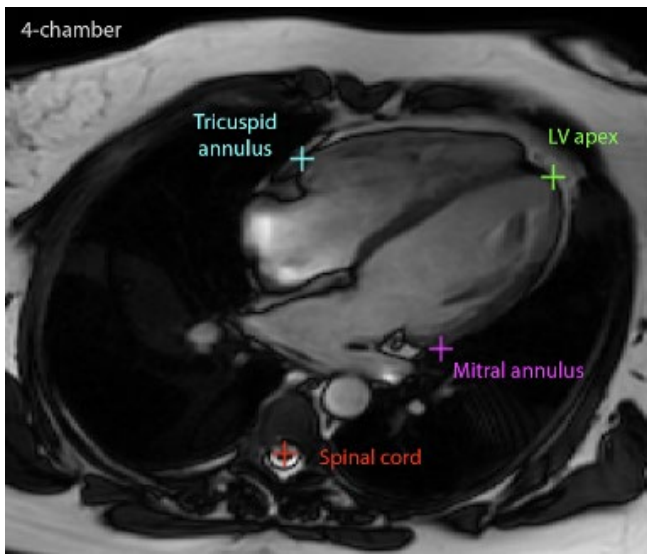












Lung Cancer

Segmentation and Diagnosis in Computed Tomography (CT)



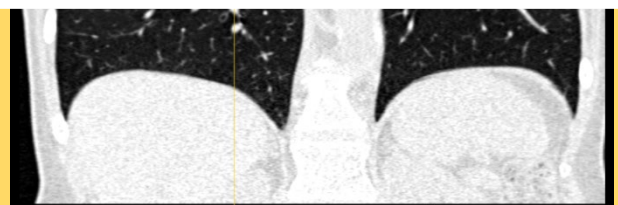
Hypothesis

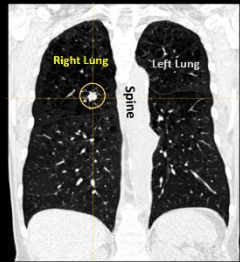
Quantitative imaging



Disease classification can be *predicted by machine learning* of imaging features from tumor and surrounding tissue environment.

performance over QICs extracted from only the pulmonary nodule.





Higher quality
training
dataset

363 subjects
74 malignant
289 benign

Nodule and
Perinodular

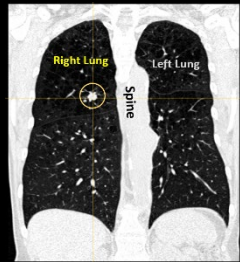
Automated
Extraction of
Imaging
Characteristics

Quantitative Imaging Characteristics for Risk Assessment from the Tumor and its

Environment
or
QIC-RATE

Reduction and
Selection

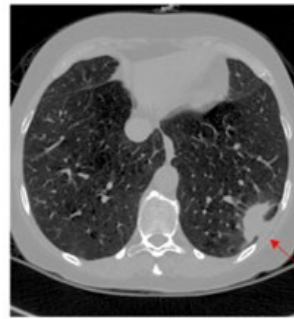
Training of neural net
ensemble for
classification



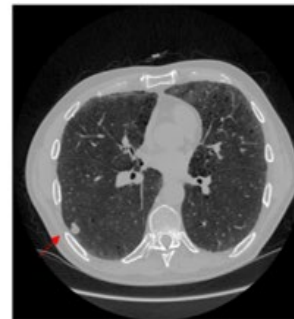
**High-res qCT
Training
Cohort:**

**363 subjects
74 malignant
289 benign**

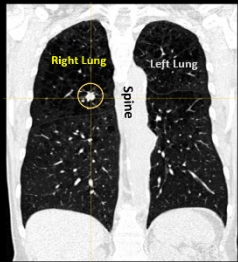
Malignant



Benign

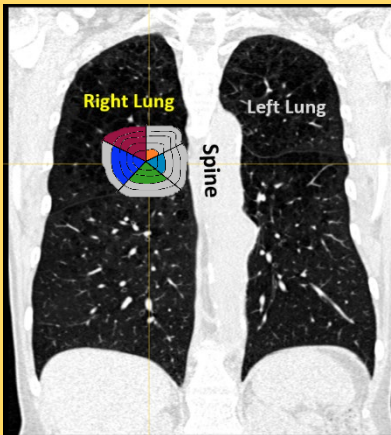


- Standardized protocols of acquisition, reconstruction
- Subjects were coached to inspiratory volume
- Slice-thickness between 0.6-1.3mm



High-res qCT training cohort:
363 subjects
74 malignant
289 benign

Nodule and Perinodular Identification



- Automatic segmentation of lung parenchyma
- Single-click seed-point of nodule
- Diameter-based dilation of nodule to include size-standardized perinodular signal

Quantitative Imaging Characteristics
Extended+

Reduction & Selection

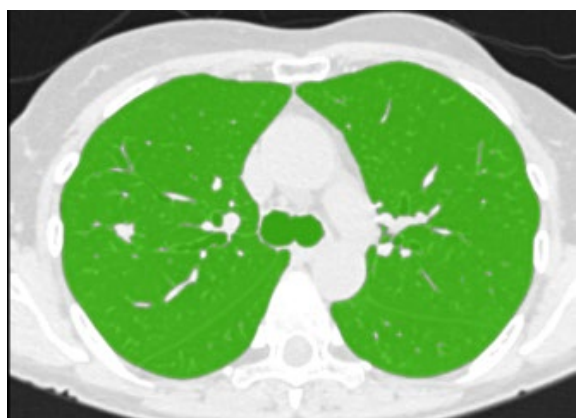
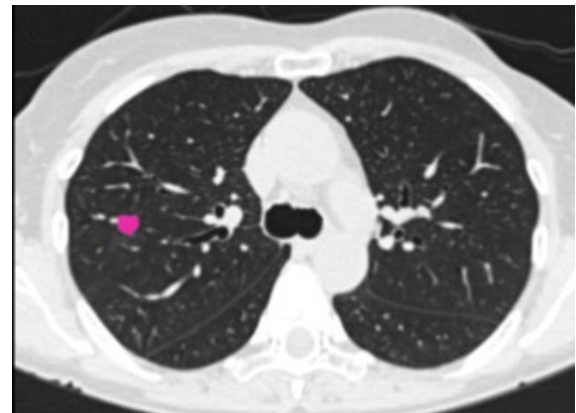
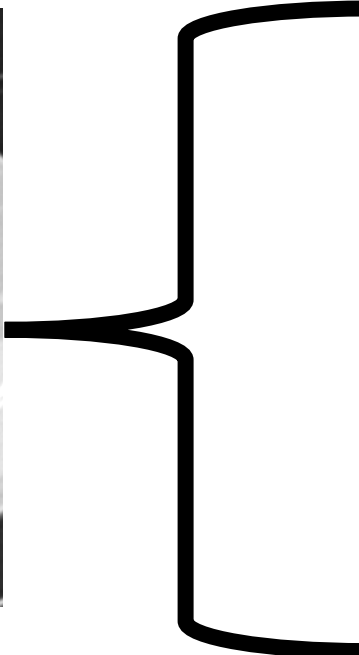
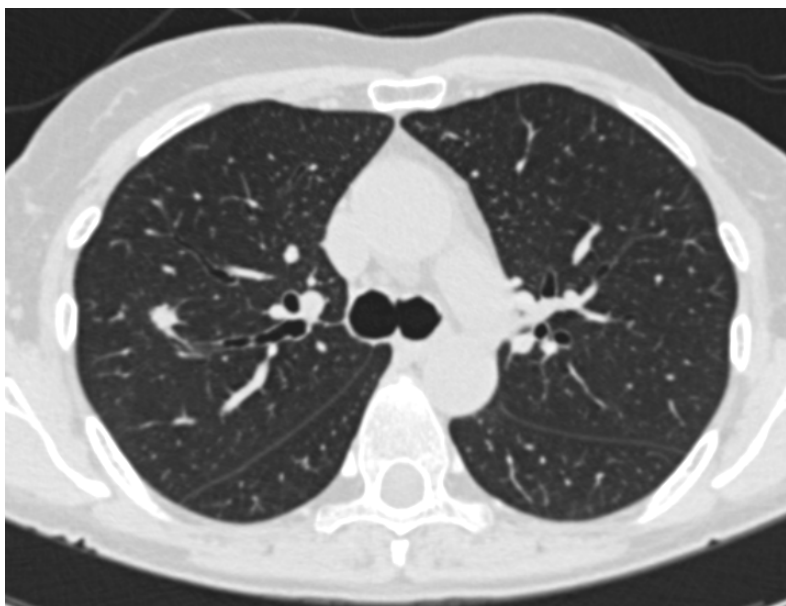
Extended

Training of neural net
Noduleole for
Classification

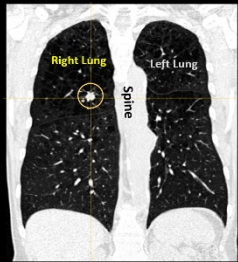
Margin

Immediate

GOAL: Semi-automated segmentation of (1) lung tumors and (2) lung tissue in computed tomography (CT)



- Random Forest classification (Lecture 4)
- Active contour shape (unsupervised learning, PCA)
- Graph-cuts segmentation (Special Clustering material Lecture 8)



High-res CT
training
cohort:

363 subjects
74 malignant
289 benign

QIC Group

Intensity Histogram *

Law's Texture *

Run Length Gray Level Texture *

Gray Level Size Zone Texture *

Neighborhood Gray Tone
Difference Texture *

Border Centroid Radial Rays

Border Absolute Sphere
Comparison

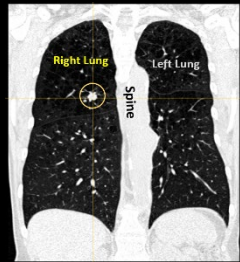
Shape and Size

Automated
Extraction of
Quantitative
Imaging
Characteristics

Reduction and
Selection

Training of neural net
ensemble for
classification





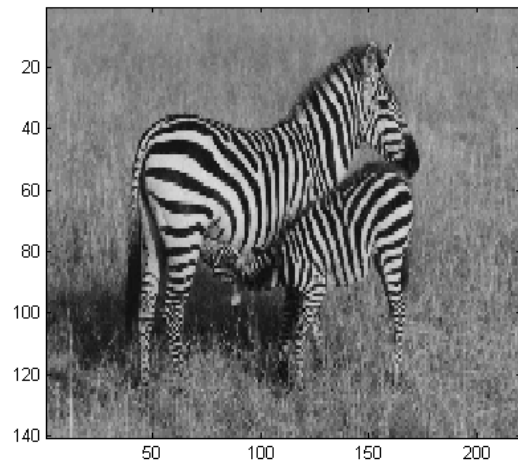
High-res CT training cohort:
363 subjects
74 malignant
289 benign

QIC Group	Description
Intensity Histogram *	Non-spatial variations in gray-level
Law's Texture *	Kernel-based texture detecting convolutions of levels, edges, spots, waves, and ripples
Run Length Gray Level Texture *	Capture coarseness of texture in a direction
Gray Level Size Zone Texture *	Capture homogeneity, non-periodic, or speckle-like texture
Neighborhood Gray Tone Difference Texture *	Heuristic-based renderings of texture
Border Centroid Radial Rays	Edge characteristics from rubber-band straightening
Border Absolute Sphere Comparison	Comparison of mask border to sphere of equal volume
Shape and Size	Physical-space attributes

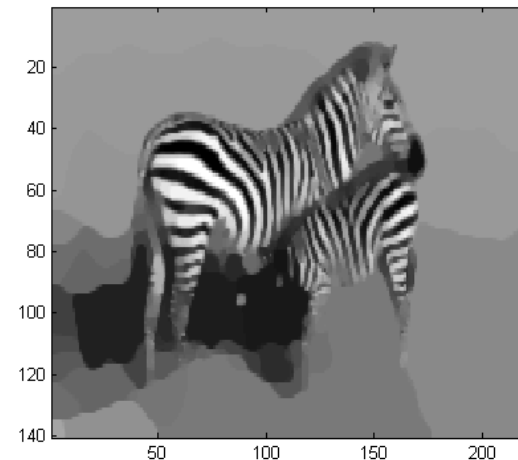


Group	Description	# features
Intensity Histogram *	Non-spatial variations in gray-level	14
Law's Texture *	Kernel-based texture detecting convolutions of levels, edges, spots, waves, and ripples	136
Run Length Gray Level Texture *	Capture coarseness of texture in a direction	13
Gray Level Size Zone Texture *	Capture homogeneity, non-periodic, or speckle-like texture	13
Neighborhood Gray Tone Difference Texture *	Heuristic-based renderings of texture	5

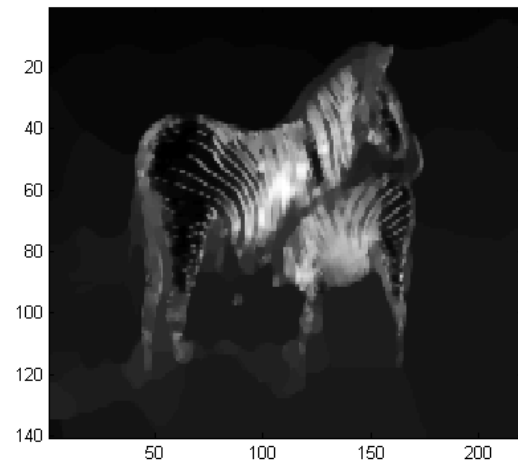
original image



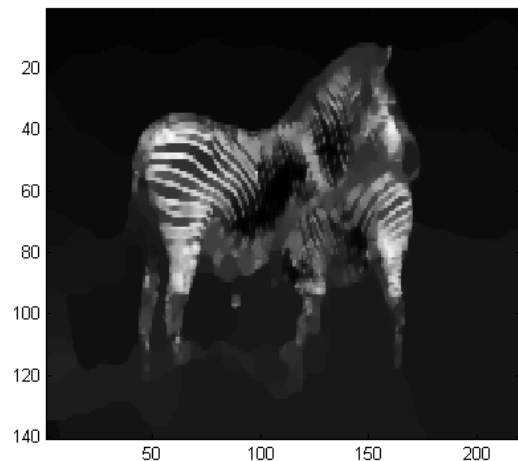
F1



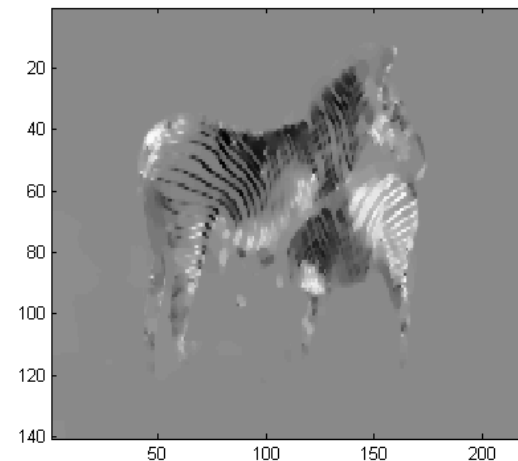
F2



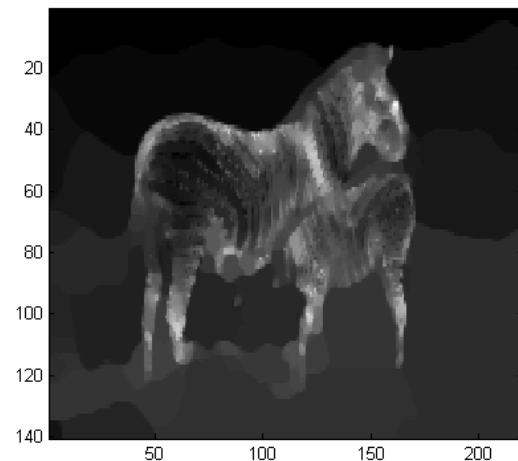
F3



F4



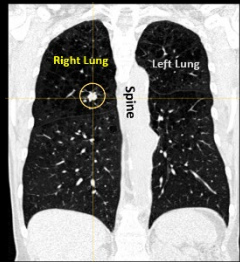
F5



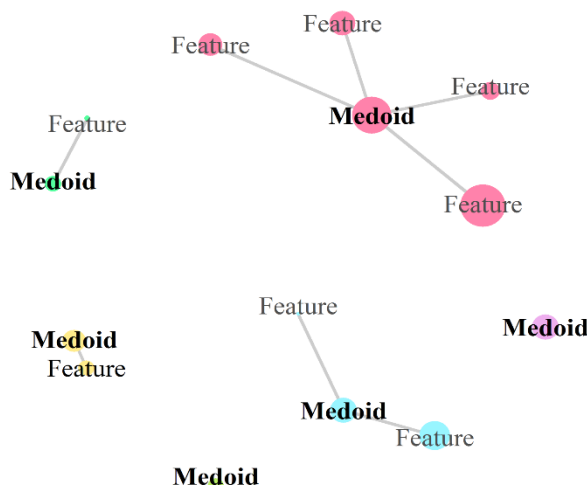
Group	Description	# features
Intensity Histogram *	Non-spatial variations in gray-level	14
Law's Texture *	Kernel-based texture detecting convolutions of levels, edges, spots, waves, and ripples	136
Run Length Gray Level Texture *	Capture coarseness of texture in a direction	13
Gray Level Size Zone Texture *	Capture homogeneity, non-periodic, or speckle-like texture	13
Neighborhood Gray Tone Difference Texture *	Heuristic-based renderings of texture	5
Border Centroid Radial Rays	Edge characteristics from rubber-band straightening	6
Border Absolute Sphere Comparison	Comparison of mask border to sphere of equal volume	5

Group	Description	# features
Intensity Histogram *	Non-spatial variations in gray-level	14
Law's Texture *	Kernel-based texture detecting convolutions of levels, edges, spots, waves, and ripples	136
Run Length Gray Level Texture *	Capture coarseness of texture in a direction	13
Gray Level Size Zone Texture *	Capture homogeneity, non-periodic, or speckle-like texture	13
Neighborhood Gray Tone Difference Texture *	Heuristic-based renderings of texture	5
Border Centroid Radial Rays	Edge characteristics from rubber-band straightening	6
Border Absolute Sphere Comparison	Comparison of mask border to sphere of equal volume	5
Shape and Size	Physical-space attributes	6

Group	Description	# features
Intensity Histogram *	Non-spatial variations in gray-level	14
Law's Texture *	Kernel-based texture detecting convolutions of levels, edges, spots, waves, and ripples	136
Run Length Gray Level Texture *	Capture coarseness of texture in a direction	13
Gray Level Size Zone Texture *	Capture homogeneity, non-periodic, or speckle-like texture	13
Neighborhood Gray Tone Difference Texture *	Heuristic-based renderings of texture	5
Border Centroid Radial Rays	Edge characteristics from rubber-band straightening	6
Border Absolute Sphere Comparison	Comparison of mask border to sphere of equal volume	5
Shape and Size	Physical-space attributes	6
		198 Tumor
		* 181 Surrounding



Nodule and K-medoids Clustering Visualization



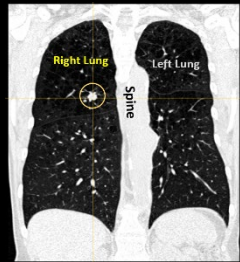
High-resolution training cohort
363 subjects
74 malignant
289 benign

Automated Extraction of Quantitative Imaging Characteristics

Reduction and Selection

Training of neural net ensemble for classification

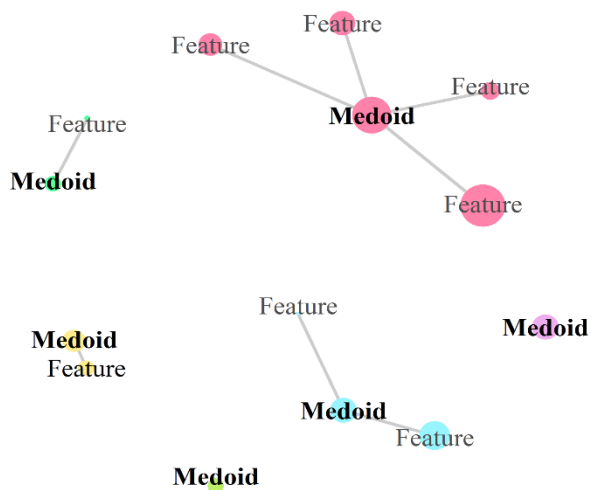




Nodule and K-medoids Clustering Visualization

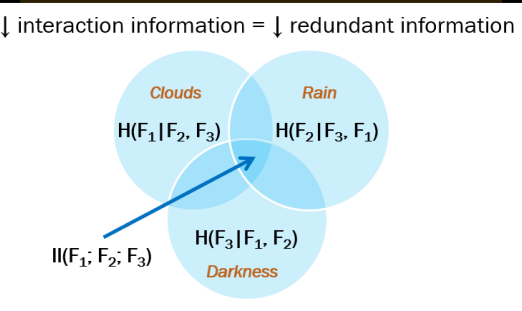
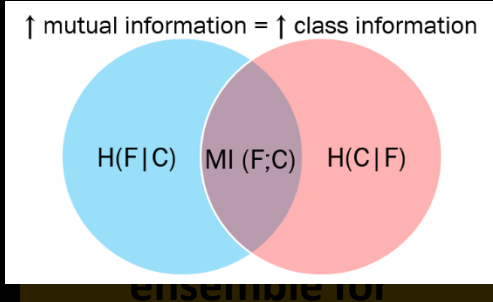
High-resolution training cohort

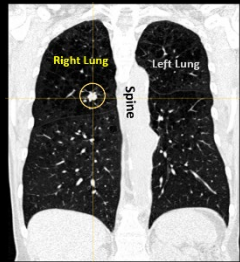
363 subjects
74 malignant
289 benign



Automated Extraction of Quantitative Imaging Characteristics

Reduction and Selection

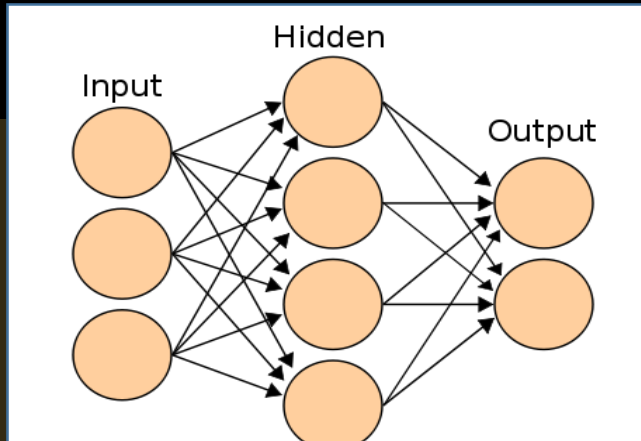




High-res qCT
training cohort:

363 subjects
74 malignant
289 benign

- Training performance measured through 10-fold cross validation
- Hyper-parameters (learning rate, momentum, weight initialization, decay, etc.)



Kidney Kidney

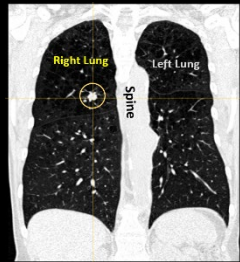
Automated
Extraction of
Quantitative
Imaging
characteristics

Reduction and
Classification



Training of neural net
ensemble for
classification

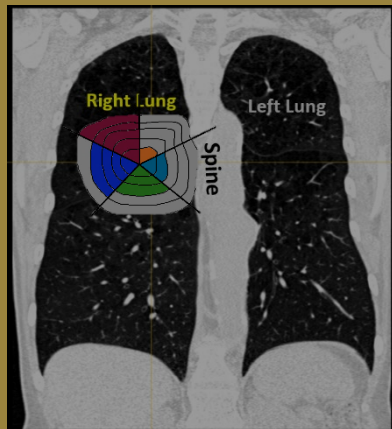
- Support Vector Machine (SVM)
- Linear Discriminant Analysis (LDA)
- Decision Trees & Random Forest



High-res qCT
Training
Cohort

363 subjects
74 malignant
289 benign

Nodule and Perinodular identification



Automated
Extraction of
Quantitative
Imaging
Characteristics

Reduction and
Selection

50 QICs

Training of neural net
ensemble for
classification

Extended QIC-RATE
AUC-ROC: 1.0;
AUC-PR: 0.945

Validation on
independent cohort



Beyond simple
cancer/non-cancer
classification?

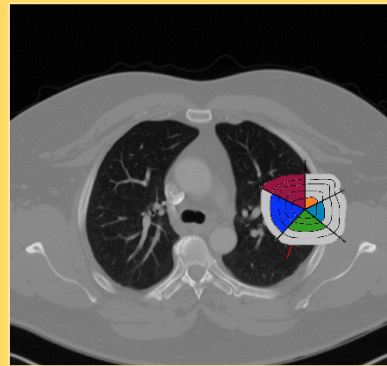
Histoplasmosis vs NSCLC



Clinical cohort

71 subjects
40 NSCLC
31 Histo

Nodule and
Perinodular
identification



Automated
Extraction of
Quantitative
Imaging
Characteristics

Reduction and
Selection

10 QICs

Training of neural net
ensemble for
classification

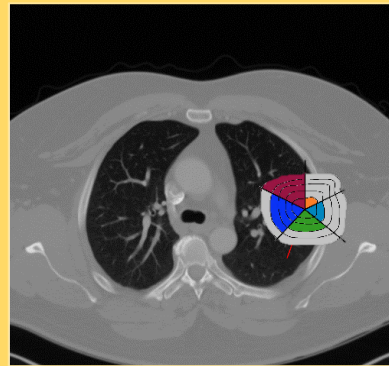
Extended+ QIC-RATE
AUC-ROC: 0.89

Histoplasmosis vs NSCLC



Clinical cohort
71 subjects
40 NSCLC
31 Histo

Nodule and
Perinodular
identification



Automated
Extraction of
Quantitative
Imaging
Characteristics

Reduction and
Selection
10 QICs

Training of neural net
ensemble for
classification

Extended+ QIC-RATE
AUC-ROC: 0.89

Comparison to
human observers

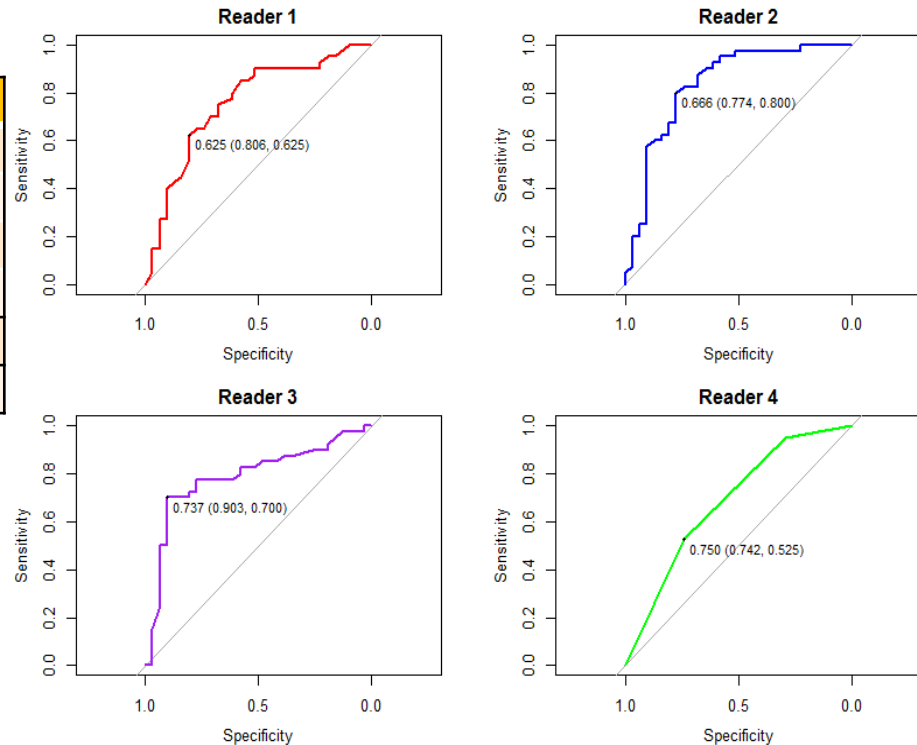


Comparison to human observers

	AUC-ROC	Sensitivity	Specificity
Reader 1	0.76	0.88	0.62
Reader 2	0.80	0.79	0.73
Reader 3	0.74	0.65	0.88
Reader 4	0.65	0.94	0.31
Average Reader	0.74	0.82	0.63
Extended+	0.89	0.83	0.84

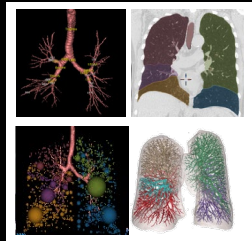
Agreement among readers:

- Interclass Correlation Coefficient = 0.52
- Weighted Cohen Kappa = 0.49



Beyond texture and
intensity features?

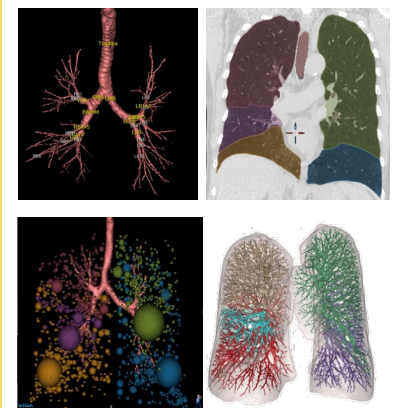
Relationship Lung Cancer and COPD



High-res qCT
Training
Cohort

278 subjects
71 malignant
207 benign

Apollo Extraction of Quantitative Imaging Characteristics



Reduction and Selection

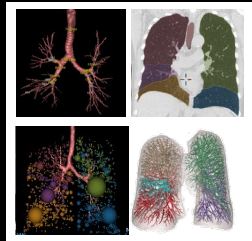
17 QICs

Training of neural net ensemble for classification

Imaging QIC-RATE
AUC-ROC: 0.74



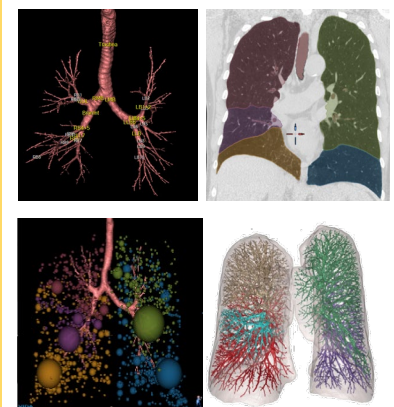
Relationship Lung Cancer and COPD



High-res qCT
Training
Cohort

278 subjects
71 malignant
207 benign

Apollo Extraction of Quantitative Imaging Characteristics



Reduction and Selection

17 QICs

Training of neural net ensemble for classification

Imaging QIC-RATE
AUC-ROC: 0.74

Comparison to multivariate mathematical prediction model



K-medoids Clustering Visualization

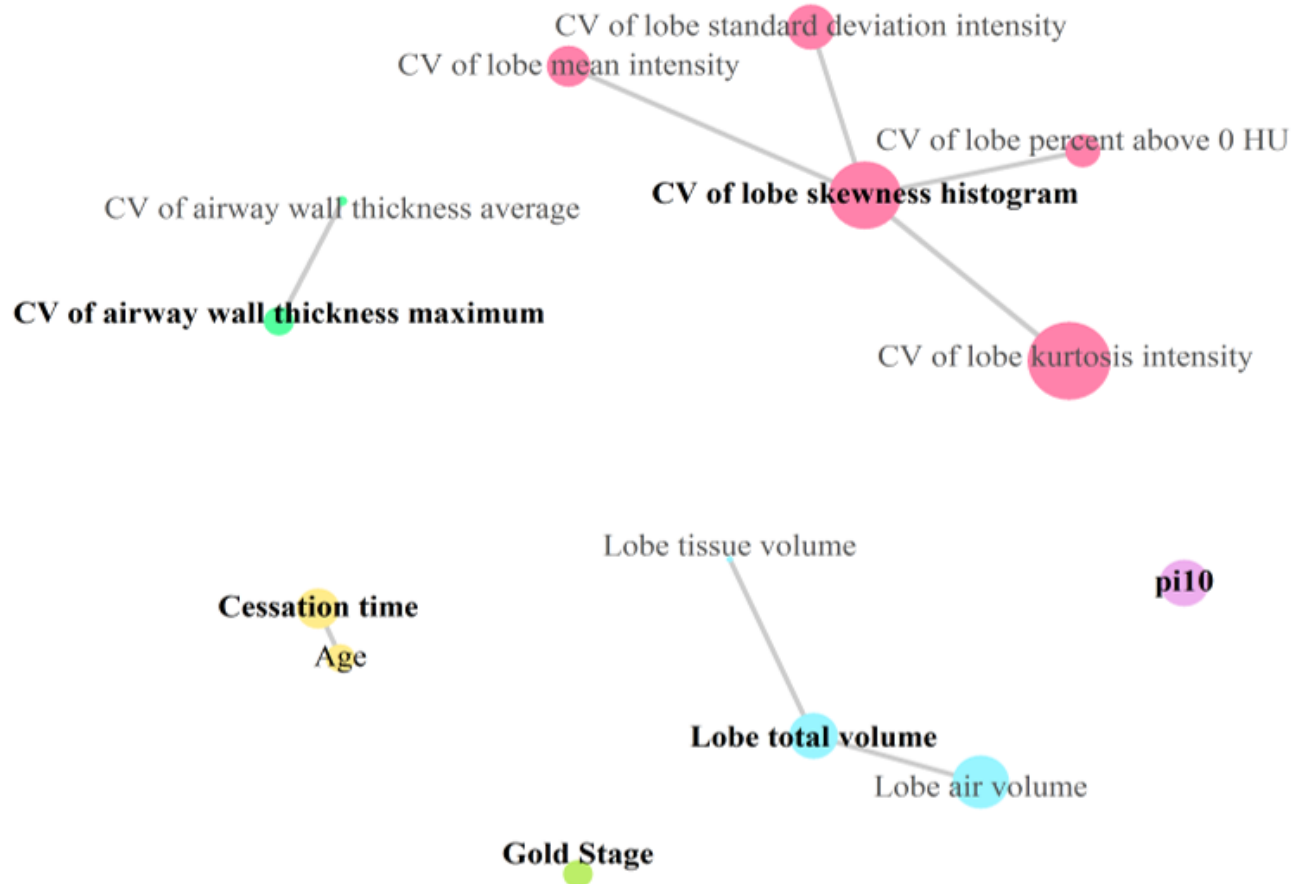
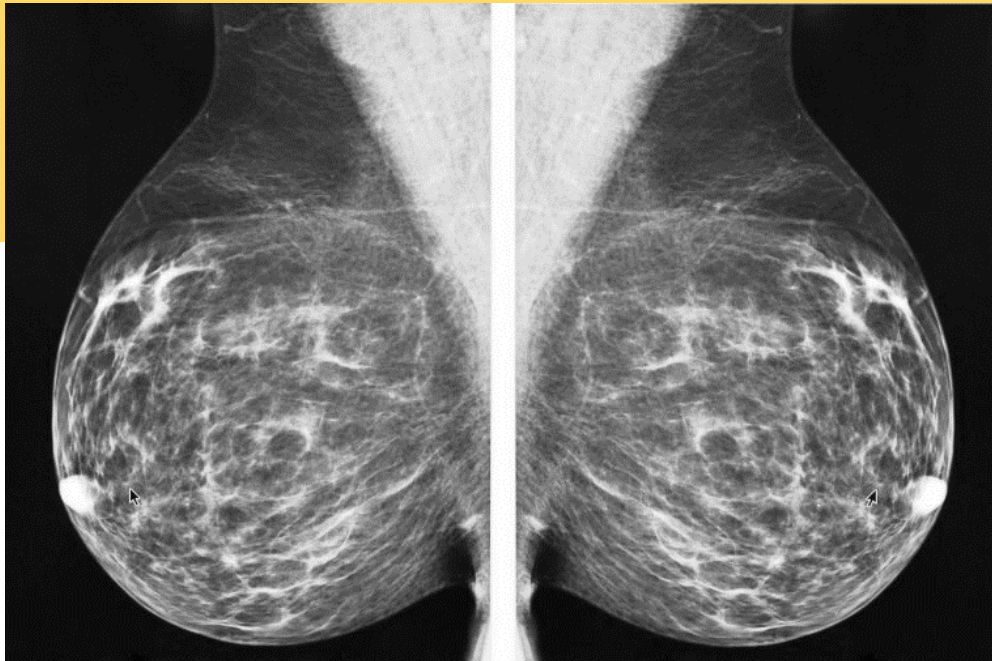


Figure 7.1

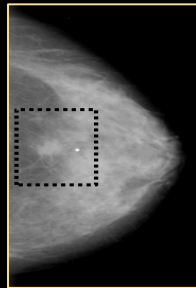
Beyond the lung and CT
imaging?

Breast Cancer

Segmentation and Diagnosis in Mammography (MG)



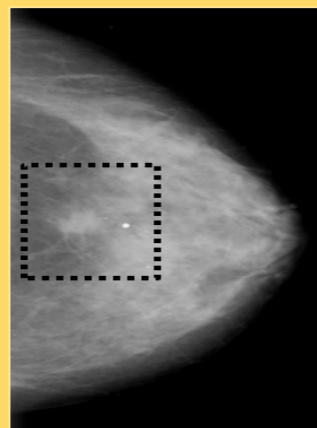
Breast Cancer in Mammography



Publicly available dataset

1000 subjects
507 malignant
493 benign

Tumor and Perinodular identification



Automated Extraction of Quantitative Imaging Characteristics

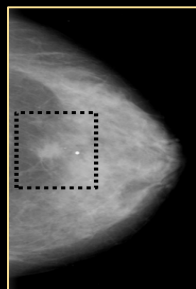
Reduction and Selection

38 QICs



Training of neural net ensemble for classification

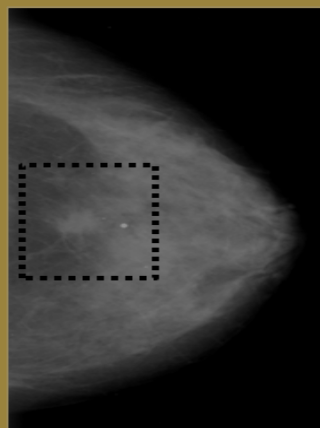
Margin QIC-RATE
AUC-ROC: 0.967



Publicly available dataset

1000 subjects
507 malignant
493 benign

Nodule and Perinodular identification



Automated Extraction of Quantitative Imaging Characteristics

Reduction and Selection

38 QICs

Training of neural net ensemble for classification

Margin QIC-RATE
AUC-ROC: 0.967

Comparison to other machine learning approaches



Comparison to other machine learning approaches

Publication	Cohort	AUC-ROC	Accuracy	Sensitivity	Specificity
Xie ¹	330	0.966	96.0	96.3	94.3
Abbas ²	350	0.910	91.0	92.0	84.2
Verma ³	200	NR	93.5	97.8	90.7
Jaffar ⁴	1800	0.910	93.0	92.8	91.4
Zhang ⁵	681	NR	84.4	NR	NR
QIC-RATE	1000	0.967	0.90	0.86	0.95
Validation	115	NR	0.82	0.87	0.76

1 – Xie, 2015, *Neruocomputing*

2 – Abbas, 2016, *Computers*

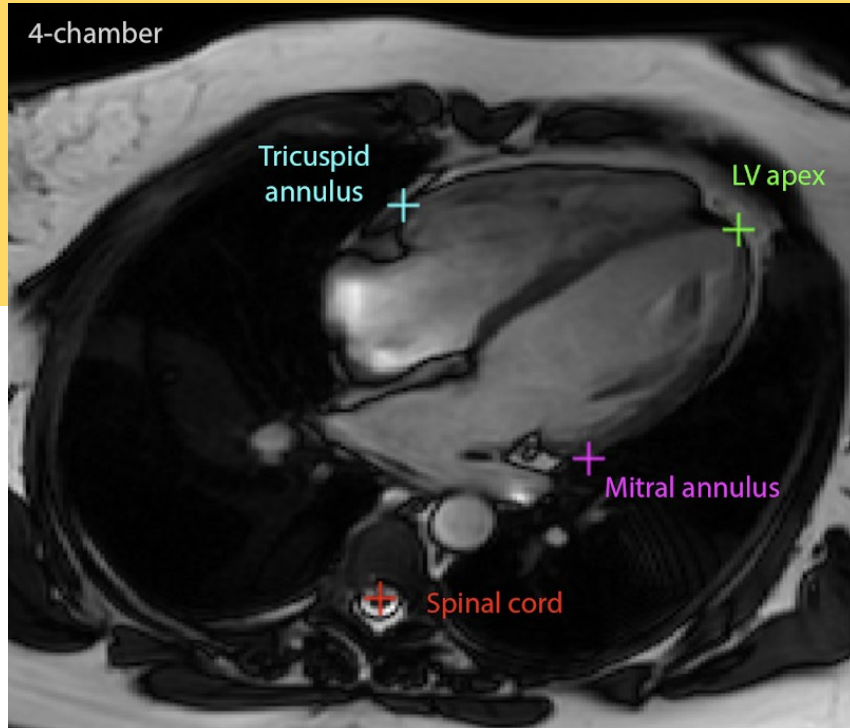
3 – Verma, 2009, *Pattern Recognition*

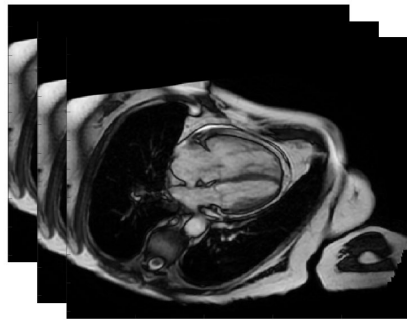
4 – Jaffar, 2017, *Advanced Computer Science and Applications*

5 – Zhang, 2009, *MICCAI Proceedings*

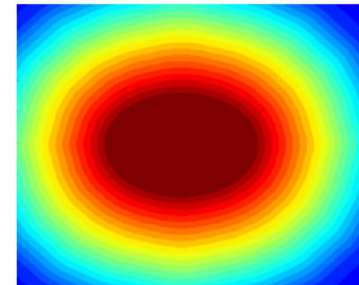
Pulmonary Hypertension

Diagnosis and Prognosis in Magnetic Resonance Imaging (MRI)

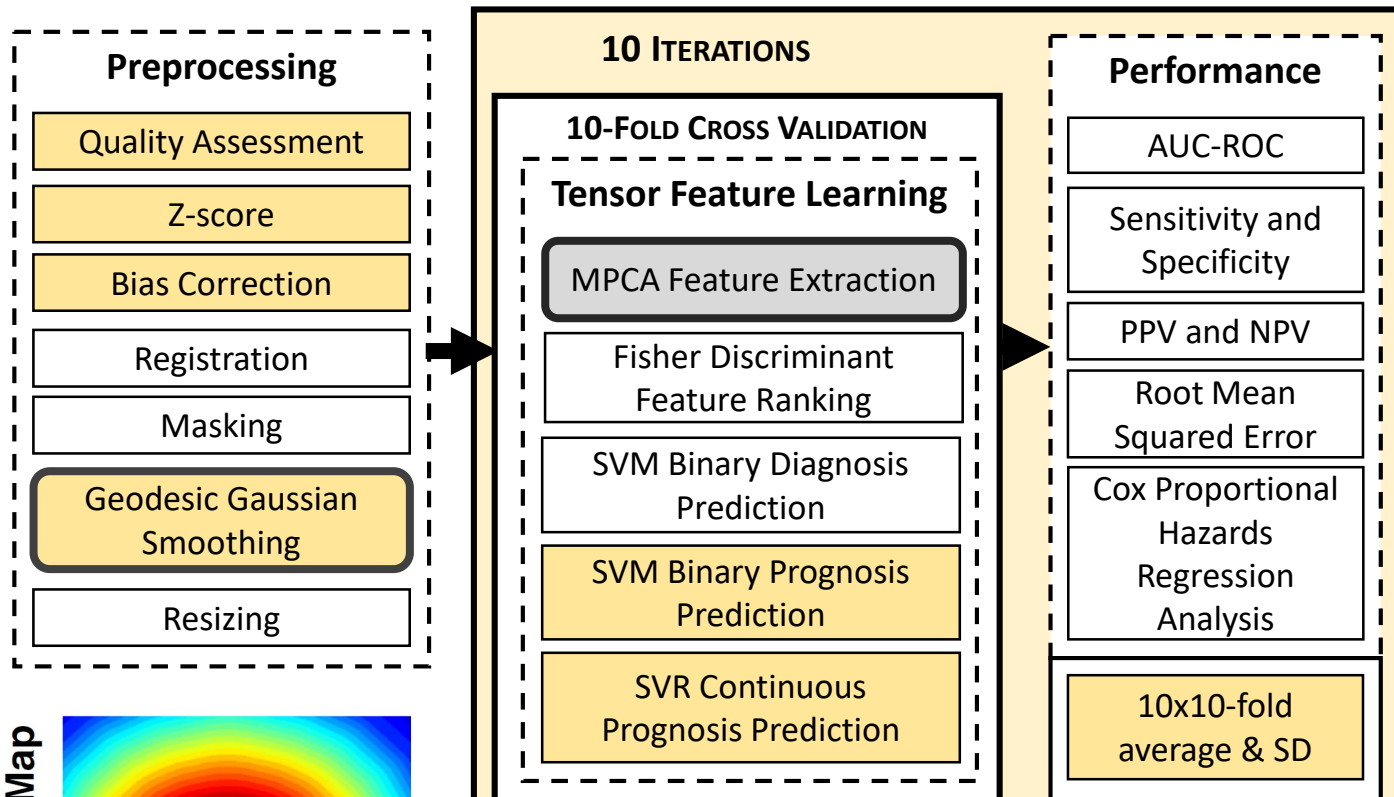




Geodesic Map



Uthoff, MICCAI, 2020.



MPCA = multilinear principal component analysis

SVM = support vector machine

PPV = positive predictive value

NPV = negative predictive value

AUC-ROC = area-under receiver-operator characteristic curve

SVR = support vector regression

SD = standard deviation

Lessons Learned

- Start with a clinical question or application
 - DATA DATA DATA!
- Feasibility and state of the art
- Adaptation of developed tools, development of modular tools

Lecture Recap

1. My Journey
2. Medical Imaging
3. Applications
 1. Lung Cancer (CT)
 2. Breast Cancer (MG)
 3. Pulmonary Hypertension (MRI)
4. Considerations

